Author Manuscript

Author Manuscript

Author Manuscript

Author Manuscript

HHS Public Access

Author manuscript

Appl Radiat Isot. Author manuscript; available in PMC 2017 August 30.

Published in final edited form as:

Appl Radiat Isot. 2017 April ; 122: 211–214. doi:10.1016/j.apradiso.2017.01.037.

A simple thick target for production of ^{89}Zr using an 11 MeV cyclotron

Jeanne M. Link[a,*,1], **Kenneth A. Krohn**[a], and **Matthew J. O'Hara**[b]

[a]Molecular Imaging Research, Box356004, Department of Radiology, University of Washington, 1959 NE Pacific Street, Seattle, WA 98195-6004, USA

[b]Radiochemical Science & Engineering Energy & Environment Directorate, Pacific Northwest National Laboratory, 902 Battelle Boulevard, Richland, WA 99352, USA

Abstract

The growing interest but limited availability of ^{89}Zr for PET led us to test targets for the ^{89}Y(p,n) reaction. The goal was an easily constructed target for an 11 MeV Siemens cyclotron. Yttrium foils were tested at different thicknesses, angles and currents. A 90° foil tolerated 41 μA without damage and produced ~800 MBq/h, > 20 mCi, an amount adequate for radiochemistry research and human doses in a widely available accelerator. This method should translate to higher energy cyclotrons.

Keywords

^{89}Zr production; 11 MeV production; Target; Experimental yields; RDS Eclipse

1. Introduction

Zirconium-89 is a positron emitting radionuclide with a half-life of 78.4 h. We first produced ^{89}Zr on a biomedical cyclotron and described its potential as a useful radionuclide for PET antibody imaging at the 3rd International Symposium on Radiopharmaceutical Chemistry in Boston (Link, 1986). In recent years, the use of ^{89}Zr has increased significantly, particularly as a radiolabel for antibodies where a several-day half-life is required (Link et al., 1986; DeJesus and Nickles, 1990; Fischer et al., 2013; Holland et al., 2009; Meijs et al., 1992, 1997; Borjesson et al., 2006; Zhang et al., 2011; Bhattacharyya et al., 2013). The most common method for production of ^{89}Zr uses a cyclotron and the ^{89}Y(p,n) ^{89}Zr reaction (Sadeghi et al., 2012) and the cross sections for this production have been reported by many investigators including Levkovskii (1991); Wenrong et al. (1992); Uddin et al. (2005); Omara et al. (2009); Sadeghi et al. (2012); Kakavand and Taghilo (2013); and for the ^{89}Y(d,2 n) ^{89}Zr reaction by Zweit et al. (1991). Despite the increasing use of this radionuclide, production has been limited to a few centers that have specialized targets for cyclotrons of ≥ 15 MeV. The purpose of the work presented here was

*Corresponding author. lijea@OHSU.edu (J.M. Link).

[1]Present/Permanent address: Diagnostic Radiology, Center for Radiochemistry Research, Mailcode L104, Oregon Health & Science University, 3181 SW Sam Jackson Park Road, Portland, Oregon 97239.

Author Manuscript Author Manuscript Author Manuscript Author Manuscript

to develop and evaluate alternative targets for production of ^{89}Zr with the goal of a target that was easily made and could withstand reasonably high beam currents using natural yttrium targets to obtain multi-millicurie yields of ^{89}Zr.

2. Methods

Yttrium metal foils with thicknesses of 0.1, 0.25, 0.50 and 1.0 mm, and 99.9% purity were obtained commercially (Sigma-Aldrich, Alfa Aesar, Fluka and ESPI) and used as provided. Yttrium oxide was obtained from Sigma-Aldrich. Helium gas was research grade. The cyclotron used was a Siemens Eclipse with 11 MeV proton beam.

A 4-position Siemens Eclipse target holder or “carousel” was used for holding the Zr-targets that were tested. A 25 μm thick aluminum window separates targets mounted in the carousel from the cyclotron vacuum tank. The proton beam on target after passing through the aluminum window was nominally 10.7 MeV based on stopping power calculations (Ziegler and Littmark, 1980).

All targets were machined from 6061-T6 aluminum rod that was milled to fit into a Siemens Eclipse cyclotron modified Faraday cup “paper burn” unit. The Siemens paper burn unit consists of two parts. The outside of the unit is a hollow cylinder, essentially a Faraday cup, that is water-cooled on the outside (Fig. 1). A smaller cylinder, 2.05 cm diameter by 7.6 cm long, with a paper attached to the front, inserts tightly into the hollow cavity of the paper burn unit and is irradiated at low current to qualitatively assessing beam shape. We also irradiated nickel instead of paper to make radioactive copper. We imaged the irradiated material using a BioRad phosphor imager to obtain quantitative images of the beam profile (Fig. 2). The beam is approximately 3 mm × 3 mm beam and gaussian.

New aluminum inserts for the hollow cylinder part of the paper burn unit were made to hold yttrium foils or yttrium oxide and the inserts were the same diameter, 2.05 cm, as the paper burn insert for at least part of the length of the insert. The inserts that were tested ranged from 6.5 to 7.5 cm in length with a flat section ~ 5 mm wide milled off the top of the insert to allow helium gas to escape. Four target insert designs were tested to make ^{89}Zr (Fig. 1). One was a target with a 12° angle to the incident proton beam with a rectangular aluminum carrier having sides 2 mm high to hold yttrium oxide powder that was pressed by hand. The powder was covered by a foil of 0.17 mil Arnavar® foil to prevent powder loss. Aluminum inserts (targets) for irradiating solid yttrium metal foils had 12°, 24°, or 90° angles to the beam to test the value of spreading the beam area to reduce current density (watts.cm^{-2}) on the yttrium metal (Fig. 1). For each target, helium gas was passed through a 1/8″ line fitted into the side of the main hollow cylinder piece and used for cooling of the yttrium target insert. The yttrium target inserts were cooled using helium passed over the foils at a rate of 300–500 cm^3 min^{-1}. Irradiations on the yttrium targets used times ranging between 15 and 60 min with varying beam currents on target.

After irradiation we typically waited at least 20 min before removing the target from the hollow cylinder. The irradiated yttrium was measured using calibrated ion chambers (Capintec, Ramsey, NJ) until measurements of the half-life showed that only ^{89}Zr remained.

Author Manuscript Author Manuscript Author Manuscript Author Manuscript

Low level counting using a Cobra II counter (Packard) with a 3″ detector and MCA detection was used to search for other radionuclides by studying photopeaks or counting over sufficient time to evaluate decay curves for more than one component.

The Siemen's Eclipse tunes the beam for each run at low current on target. In order to determine the total amount of current that was put on the yttrium target, current was logged every second from the start of low current beam tuning on target and through the total irradiation irradiation. Total integrated beam was the sum of this logged current. Average beam on target was calculated as the total current divided by time irradiated. Typical tuning time was 2 min at 10 μA.

We measured the fraction of the beam lost to the aluminum clamps holding the yttrium material in each target by comparing the yield in mCi/uA h at end of bombardment (EOB) from a direct 90° irradiation on a thick-to-beam unclamped piece of Y metal in the paper burn position with the yield on targets with clamps that intercepted some of the beam. Beam current for these tests was between 10 ot 20 μA on the Y foil to avoid any warping or loss from the foils. The fraction of beam current that was estimated by this method to actually reach the Y foil compared with the aluminum clamps on the clamped targets and the losses to the back of the target from thin to beam foils is called effective current for the remainder of this manuscript.

The difference in yield for one 0.25 mm foil compared with thick to beam 2×0.25 mm Y foils was also measured.

3. Results

The yttrium target irradiations produced trace amounts of ^{13}N from oxygen on the surface of the yttrium, along with $^{89\,m}Zr$ (T1/2 4.16 min) and the desired ^{89}Zr. No other radionuclides were detected out to 6 half-lives of the ^{89}Zr.

The Y_2O_3 target did not transfer heat well and showed melting in the center with only 12 μA on target and, as expected, had lower measured yields 12.2 MBq/μA h (0.33 mCi/μAh) at end of bombardment (EOB) compared with yttrium metal. We did not perform further evaluation of Y_2O_3 targets.

Multiple yttrium foil thicknesses were tested. For a 10.7 MeV beam directly hitting natural ^{89}Y foils we calculated that 0.47 mm thick of yttrium foil would reduce the energy of the proton beam to 4.0 MeV, reducing the cross section from 700 to 850 mb at 10.7 MeV to < 20 mb (Zeigler and Littmark, 1980; Sadeghi et al., 2012). Stacks of 0.1 mm foils totaling 0.5 mm were tested but the foils did not transfer heat well enough to the next foil, even with compression to improve contact and the foils were vaporized through the center. This was anticipated due to lack of convective gas cooling in the middle layers and the poor conductivity between neighboring foils. Irradiation of one mm thick Y foils did not sustain as high a current on target as other single foils because the center of the target warped due to insufficient heat removal. Most experiments used 0.25 mm yttrium foils and both single and double 0.25 mm foils, for a thick production target, were tested.

Author Manuscript Author Manuscript Author Manuscript Author Manuscript

Yields from 43 irradiations of the Y targets that did not melt are presented in Table 1 as a function of the beam angle target. The yields for a single 0.25 mm foil were 23 ± 10 MBq/μA h for the top foil at 12°, 24.3 ± 0.6 MBq/μA h at 24° and 20.5 ± 1.1 MBq/μA h at 90°, all for one-hour irradiations. For the clamped 90° angle using double 0.25 mm yttrium foils the summed yield was 23.3 ± 2.2 MBq/μA h. The measured yield on the 12° target had a large variation because a small change in beam tune or the clamping of the target inserts among runs moved the center of the beam a large distance up or down or to the side with the shallow angle.

The maximum beam that could be put on the targets differed for the different beam angle targets. For single foil irradiations, only 25 μA could be put on the 24° target before the foil showed heat damage. The 12° single foil could withstand 35 μA without showing heat damage. The 90° foil tolerated 41 μA of beam before there was visible heat damage (Table 1). The foil areas were quite different for the different targets and the 12° foil target could only sustain 31 W cm^{-2} (35 μA), 24° only 56 average watts cm^{-2} and the 90° target 439 W cm^{-2} (Table 1). This translated to yields of 805, 608 and 841 MBq per 1 h run at maximum current for the 12°, 24° and 90° targets respectively.

4. Discussion

The thick target yield in MBq/μA h from our dual foil targets agreed well with the theoretical thick target yield for the ^{89}Y (p, n) ^{89}Zr reaction using different models reported by Sadeghi et al. (2012) (Fig. 3) indicating that we were not losing appreciable amounts of beam. It was surprising but gratifying that in these studies the target that withstood the greatest current on the target was associated with the greatest beam density on the yttrium foil. It was anticipated that the more spread out beams would allow for greater beam current on target however the path length of protons increases greatly with more shallow angles so the beam is fully stopped in the yttrium. Other practical reasons for the results were probably a combination of the stronger clamping of the foils to the target body for the 90° target and more dense helium cooling on the smaller foil area. The helium gas was more focused on the 90° foil because there was less space for the helium in the target cavity. The minimal space in the target allowed for only limited clamping on the sides for the 12° and 24° targets. The 90° target used a two-screw washer clamp with the ring pressing down on the full perimeter of the target face to provide good contact through the entire target foils in addition to having better helium cooling on the face of the target.

There was one disadvantage to the ring clamp; some of the beam hit the clamp rather than the yttrium. The 12° and 24° targets had similar yields in MBq/μA h but the 90° target had a yield that was only 86% of the other two targets due to some beam loss on the clamp. Earlier designs with thinner clamps gave 23.7 ± 0.5 MBq/μA h yield for the 90° target, which is not significantly different from the 12° and 24° targets but with a weaker clamp it could not withstand as much beam current. The high heat capacity of the yttrium caused the foils to raise up in the center of the foil, even though the edges were clamped, as the current exceeded the maximum tolerated value. Despite the losses due to the clamp, the 90° target gave the greatest yield and accounting for beam on the ring clamp, the effective maximum current on the yttrium was 35.5 μA. The maximum beam deposited was 211 W cm^{-2} for the

Author Manuscript Author Manuscript Author Manuscript Author Manuscript

single 90° foil (Table 1) but effective maximum current on Y foil due to the ring clamp beam loss was 183 W for a single foil and 380 W for the double foil. The use of two 0.25 mm foils rather than one 0.25 mm foil yielded 8–13% more product for all targets.

There is an additional benefit of the use of the 90° foil. With a smaller surface area, less yttrium metal can be used. The amounts of foil required for the three targets were 0.84 g for 12°, 0.34 g for 24° and 0.15 g for 90° for one 0.25 mm foil. The higher surface area target uses more yttrium that has to be separated from the ^{89}Zr and a greater amount of yttrium leads to more trace metal impurities in the foil. The primary impurity in the yttrium foil that can affect ^{89}Zr binding chemistry is iron, which also chelates with deferrioxamine, the principle chelate used for ^{89}Zr. Iron will behave like Zr so can effect the effective specific activity of the product zirconium. The amount of iron in the foils varied between 100 and 520 μg/g of yttrium and we used the yttrium foils with the least amount of iron we could find. In addition, our ion exchange separation methods remove most of the iron, and EDTA can also be used to remove the Fe before using ^{89}Zr (Baroncelli and Grossi, 1964; Schwarzenbach and Schwarzenbach, 1963). Nevertheless, a smaller foil still means less yttrium to dissolve and purify and less metal contaminants to remove or that will compete with ^{89}Zr and decrease the effective specific activity of this radionuclide.

The yields obtained were consistent with previous cross sections and yields for the ^{89}Y(p,n)^{89}Zr reaction (Sadeghi et al., 2012; Taghilo et al., 2012). The yield from the Siemens Eclipse machine is lower than for other reports because the energy on yttrium is only 10.7 MeV, which is just at the energy where the cross section for this reaction is reaching its maximum. Nonetheless, this simple method using a target that can be built in house makes it possible to obtain 840 MBq (22 mCi) in a single 1 h irradiation. This is lower than has been reported by most other investigators that ranged from 12 to 61 MBq/μA h (Sadeghi et al., 2012). However, all of those reports started with energies greater than that reported here, although many were also thin (low MeV stopping ranges) targets. This is the first report of a low energy target (10.7 MeV entrance energy) that achieves a useful production yield, and makes the production of ^{89}Zr practical for hundreds of accelerators. These results do not just apply to the 11 MeV cyclotron. Damage to the foil comes from inability to remove heat. Our cyclotron beam geometry was approximately Gaussian and about 3 mm in diameter in both the x and y directions for 87% of the beam (Fig. 2). A similar target on a PETtrace 16.5 cyclotron with a similar beam profile should have very high production rates.

For a proton beam that went from 14 MeV entrance on the yttrium through 0.50 mm of yttrium should exit with an energy of ~8 MeV but would encompass 90% of the cross section from 14 MeV to 8 MeV in energy (Ziegler and Littmark, 1980; Omara et al., 2009; Sadeghi et al., 2012, Fig. 3). For an attenuation from 15 to 8 MeV only 6 MeV would be deposited in target (6 W/μA) so that, depending on the beam shape, the target with two foils should withstand 56 μA of current on target (48 μA on the Y foils) and give a yield of approximately 90% of the 58 MBq/μA h theoretical yields (Omara et al., 2009) or 2.9–3.7 GBq at EOB for 48 μA on the foils (Sadeghi et al., 2012) with a 0.1 MBq impurity of ^{88}Zr (half-life 83.4 days) and this could be reduced by an entrance energy slightly lower than 14 MeV. Thick target yields in Fig. 3 show that while useful amounts of ^{89}Zr can be made

Author Manuscript Author Manuscript Author Manuscript Author Manuscript

inexpensively using the system described in this manuscript with the 10.7 MeV Siemen's cyclotron, the optimal energy for production is just under 14 MeV to have a radionuclidically pure ^{89}Zr. Use of deuterons for the (d,2 n) reaction rather than protons on yttrium, for higher energy machines with deuteron capability may be a is reasonable approach for making ^{89}Zr,

5. Conclusion

A simple target system for production of ^{89}Zr using an 11 MeV cyclotron sustained relatively high currents on a yttrium foil target perpendicular to beam. A target that is orthogonal to beam requires a target of less mass. The results from this work, although designed for a specific cyclotron system, should be applicable to higher energy cyclotron systems in terms of power per area on target and produce high yields of ^{89}Zr in a relatively small mass of yttrium. Most of the cyclotrons that are in operation are lower energy cyclotrons between 11 and 16.5 MeV and simple target solutions like this may make production of ^{89}Zr and other (p,n) reaction products more accessible to researchers without having to purchase a commercial target.

Acknowledgments

This work was supported by the U.S. Department of Energy Office of Science, Isotope Development and Production for Research and Applications (IDPRA) subprogram of the Office of Nuclear Physics, S10-RR017229 and National Institutes of Health, NCI CA042045.

We wish to thank Steven C Shoner, PhD and Eric A. Shankland, PhD for help with some of the target irradiations.

Biography

Jeanne Link, Ph.D. is Professor of Diagnostic Radiology at Oregon Health & Science University (OHSU).

References

Baroncelli F, Grossi G. The complexing power of hydroxamic acids and its effect on the behaviour of organic extractants in the reprocessing of irradiated fuels -I. The complexes between benzohydroxamic acid and zirconium, iron (III) and uranium (VI). J Inorg Nucl Chem. 1964; 27:1085–1092.

Bhattacharyya S, Kurdziel K, Wei L, Riffle L, Kaur G, Hill GC, Jacobs PM, Tatum JL, Doroshow JH, Kalen JD. 2013. Zirconium-89 labeled panitumumab: a potential immuno-PET probe for HER1-expressing carcinomas. Nucl Med Biol. 2013; 40:451–457. [PubMed: 23454247]

Borjesson PK, Jauw YW, Boellaard R, de Bree R, Comans EF, Roos JC, Castelijns JA, Vosjan MJ, Kummer JA, Leemans CR, Lammertsma AA, van Dongen GA. Performance of immuno-positron emission tomography with zirconium-89-labeled chimeric monoclonal antibody U36 in the detection of lymph node metastases in head and neck cancer patients. Clin Cancer Res. 2006; 12:2133–2140. [PubMed: 16609026]

DeJesus OT, Nickles RT. Production and purification of ^{89}Zr, a potential PET antibody label. Int J Rad Appl Inst Part A Appl Radiat Isot. 1990; 41:789–790.

Fischer G, Seibold U, Schirrmacher R, Wangler B, Wangler C. (89)Zr, a radiometal nuclide with high potential for molecular imaging with PET: chemistry, applications and remaining challenges. Molecules. 2013; 18:6469–6490. [PubMed: 23736785]

Author Manuscript Author Manuscript Author Manuscript Author Manuscript

Holland JP, Sheh Y, Lewis JS. Standardized methods for the production of high specific-activity zirconium-89. Nucl Med Biol. 2009; 36:729–739. [PubMed: 19720285]

Kakavand T, Taghilo M. Cyclotron production of ^{89}Zr: A potent radionuclide for positron emission tomography. Proceedings of the DAE Symp on Nucl Phys. 2013; 58:608–609.

Levkovskii, VN. Activation cross sections for the nuclides of medium mass region (A= 40–100) with medium energy (E= 10–50 MeV) protons and alpha particles (experiment and systematics). Inter-Vesi; Moscow, Russia: 1991.

Link JM, Krohn KA, Eary JF, Kishore R, Lewellen TK, Johnson MW, Badger CC, Richter KY. 89)Zr for antibody labeling and positron emission tomography. J Label Comp Radiopharm. 1986:1297–1298.

Meijs WE, Herscheid JD, Haisma HJ, Pinedo HM. Evaluation of desferal as a bifunctional chelating agent for labeling antibodies with Zr-89. Int J Rad Appl Instrum A. 1992; 43(12):1443–1447. [PubMed: 1334954]

Meijs WE, Haisma HJ, Klok RP, van Gog FB, Kievit E, Pinedo HM, Herscheid JD. Zirconium-labeled monoclonal antibodies and their distribution in tumorbearing nude mice. J Nucl Med. 1997; 38:112–118. [PubMed: 8998164]

Omara HM, Hassan KF, Kandil SA, Hegazy FE, Saleh ZA. Proton induced reactions on ^{89}Y with particular reference to the production of the medically interesting radionuclide ^{89}Zr. Radiochim Acta. 2009; 97:467–471.

Sadeghi M, Enferadi M, Bakhtiari M. Accelerator production of the positron emitter zirconium-89. Ann Nucl Energy. 2012; 41:97–103.

Schwarzenbach G, Schwarzenbach K. Properties of desferrioxamine. Helv Chim Acta. 1963:1390–1400.

Taghilo A, Kakavand T, Rajabifar S, Sarabadani R. Cyclotron production of (89)Zr: a potent radionuclide for positron emission tomography. Int J Phys Sci. 2012; 7:1321–1325.

Uddin MS, Hagiwara M, Baba M, Tarkanyi F, Ditroi F. Experimental studies on excitation functions of the proton-induced activation reactions on yttrium. Appl Radiat Isot. 2005; 63(3):367–374. [PubMed: 15939593]

Wenrong Z, Qingbiao S, Hanlin L, Weixiang Y. Investigation of Y-89(p, n)Zr-89, Y-89(p,2n)Zr-88 and Y-89(p, pn)Y-88 reactions up to 22 MeV. Chin J Nucl Phys. 1992; 14:7.

Zhang Y, Hong H, Cai W. PET tracers based on Zirconium-89. Curr Radiopharm. 2011; 4(2):131–139. [PubMed: 22191652]

Ziegler, JF., Littmark, U. Handbook of Range, Distributions for Energetic Ions in all Elements 6. Pergamon Press; New York: 1980. p. 285

Zweit J, Downey S, Sharma HL. Production of no-carrier-added zirconium-89 for positron emission tomography. International Journal of Radiation Applications and Instrumentation Part A Appl Radiati Isot. 1991; 42:199–201.

Author Manuscript Author Manuscript Author Manuscript Author Manuscript

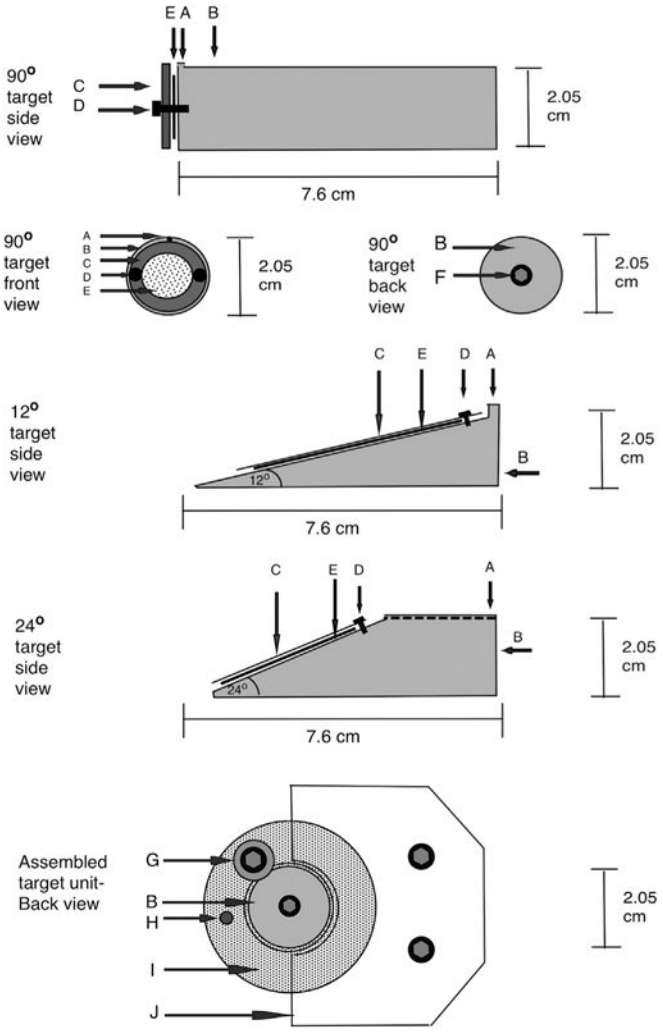

Fig. 1.

Scale diagrams of the three target inserts tested for production of ^{89}Zr using 0.5 or 0.25 mm thick Y foils. Top panel shows side, front and back views of the 90° target insert with the best performance. Middle panel shows the 12° target. The bottom panel shows side view of the 24° target. The back view for all targets were similar. The target components are labeled the same in all views. A is the position for helium gas entry into the target foil, B is the aluminum target body, C is the aluminum or steel washer or flange that held the yttrium foil against the aluminum target back. D denotes screws to tighten the flange against the aluminum back. There were two #2 screws used for the 90° target. E denotes the yttrium foil. The insert fit tightly into a water-cooled sleeve in the Eclipse target changer. Each insert had a screw mounted in the back (F) so that the insert could be pulled from the target changer quickly into a lead pig for transport. The bottom drawing shows the back of the entire mounting of the hollow cylinder with the target insert from the back. G denotes a washer and screw that is used to hold the insert (B) in place within the hollow cylinder so that the helium cooling gas does not push the insert out. H denotes the 1/8″ line for helium cooling inserted in the hollow cylinder (I) that is part of the paper beam unit. The hollow

cylinder is kept in place by the plate (J), this is a normal part of the clamping on the Siemen's target carousel.

Author Manuscript Author Manuscript Author Manuscript Author Manuscript

Author Manuscript Author Manuscript Author Manuscript Author Manuscript

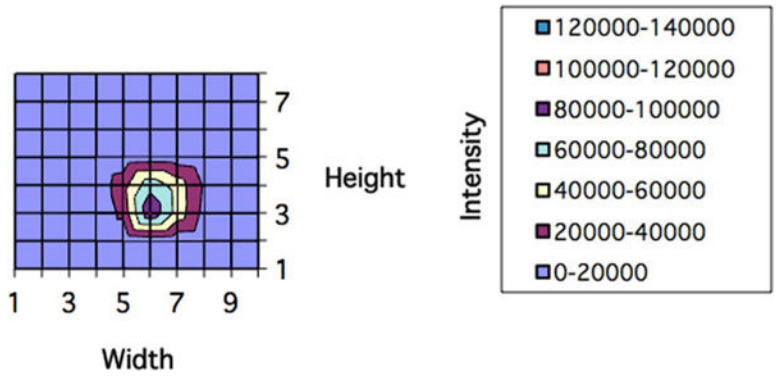

Fig. 2.

Image of quantitative beam current position and density measured by Phosphor imaging of an irradiated foil from a paper burn target. The left image shows a typical beam profile for our Siemen's Eclipse cyclotron. The picture is oriented with the height on the Y-axis and the width on the X-axis. Each square is 1 mm on a side. The right scale gives linear scale of signal intensity.

Author Manuscript Author Manuscript Author Manuscript Author Manuscript

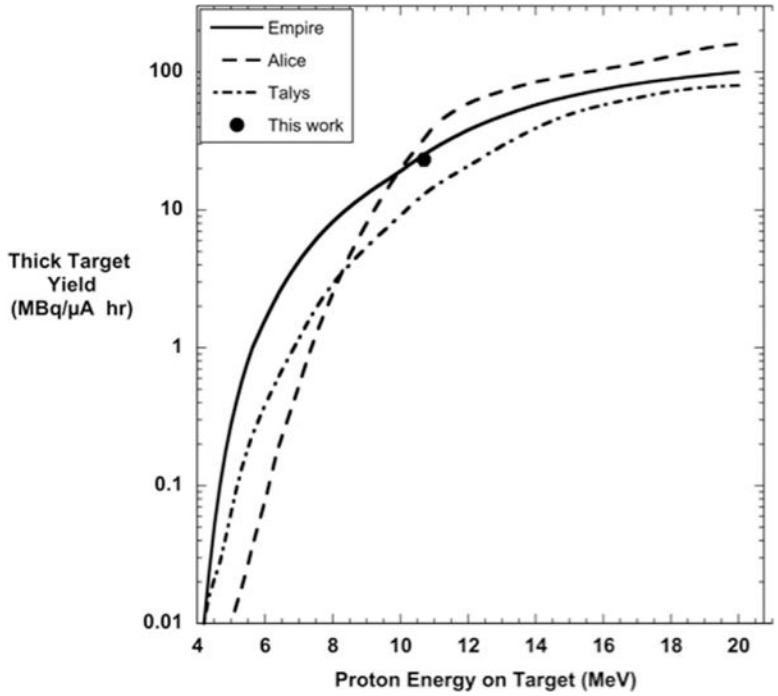

Fig. 3.

Theoretical thick target yields calculated using 3 different nuclear model codes, Empire, Alice and Talys compared with the average yield from the Eclipse 90° Y thick targets, showing that yields from the target are consistent with theoretical yields. The curves are taken directly from Sadeghi et al. (2012).

Author Manuscript

Author Manuscript

Author Manuscript

Author Manuscript

Table 1

Production results for ^{89}Zr production from various Y foil target designs using an 11 MeV proton beam. This table lists the target foil thicknesses, area (cm^2) and mass (g), maximum beam on target without damage, maximum yield in MBq/μA h, and maximum power that each target can withstand (watts cm^{-2}). The power values (watts) on target are the effective current on the Y foils corrected for loss of beam on the clamps on the 90° target. Also, the range of reported thick target yields starting at 10.7 MeV entrance energy is presented for comparison.

Target angle to beam	Yield MBq/μA h 0.25 mm thick single foil Y Avg ± std dev (n)[a]	Maximum beam withstood by target	Y Foil area (cm^2)	Beam on target (Avg. watt s cm^{-2})
	0.25 mm single Y foil			
12°	23 ± 10 (5)	35 μA	7.5	31
24°	24.3 ± 0.6 (4)	25 μA	3.0	56
90°	20.5 ± 1.1 (25)	41 μA	1.3	211 (183)
	0.50 mm double Y foil			
90°	23.3 ± 2.2 (9)	41 μA	1.3	439 (380)

[a](n) = Number of irradiations.